



# Rapid assembling organ prototypes with controllable cell-laden multi-scale sheets

Qing Gao<sup>1,2</sup> · Peng Zhao<sup>1,2</sup> · Ruijian Zhou<sup>1,2</sup> · Peng Wang<sup>1,2</sup> · Jianzhong Fu<sup>1,2</sup> · Yong He<sup>1,2</sup>

Received: 13 January 2019 / Accepted: 23 January 2019 / Published online: 5 February 2019  
© Zhejiang University Press 2019

## Abstract

A native organ has heterogeneous structures, strength, and cell components. It is a big challenge to fabricate organ prototypes with controllable shapes, strength, and cells. Herein, a hybrid method is developed to fabricate organ prototypes with controlled cell deposition by integrating extrusion-based 3D printing, electrospinning, and 3D bioprinting. Multi-scale sheets were first fabricated by 3D printing and electrospinning; then, all the sheets were assembled into organ prototypes by sol–gel reaction during bioprinting. With this method, macroscale structures fabricated by 3D printing ensure the customized structures and provide mechanical support, nanoscale structures fabricated by electrospinning offer a favorable environment for cell growth, and different types of cells with controllable densities are deposited in accurate locations by bioprinting. The results show that L929 mouse fibroblasts encapsulated in the structures exhibited over 90% survival within 10 days and maintained a high proliferation rate. Furthermore, the cells grew in spherical shapes first and then migrated to the nanoscale fibers showing stretched morphology. Additionally, a branched vascular structure was successfully fabricated using the presented method. Compared with other methods, this strategy offers an easy way to simultaneously realize the shape control, nanofibrous structures, and cell accurate deposition, which will have potential applications in tissue engineering.

**Keywords** Organ prototypes · 3D printing · Electrospinning · 3D bioprinting · Multi-scale sheets

## Introduction

Organ prototypes based on scaffolds or cell-laden structures have been widely used in tissue engineering and regenerative medicine, because they could provide carriers for cell attachment and microenvironment similar to the extracellular matrix (ECM) for cell growth [1–4]. To be close to native organs, an ideal organ prototype must mimic the structure features, cell-favorable environment, and cell distribution of the natural organs. Therefore, the corresponding requirements are put forward for the fabrication method: (1) The method should fabricate user-specific patterned structures for getting complicated tissues with controlled size

and shape; (2) the method needs to produce microscale or nanoscale fibers for simulating ECM; (3) the method enables to obtain controlled cell deposition for building complicated tissues with multiple cell types and gradient ECM.

Currently, numerous methods have been reported for the fabrication of scaffold-based organ prototypes [5–8], among which extrusion-based 3D printing is a widely used method because it can easily fabricate 3D customized structures by using thermoplastic biodegradable polymers, such as polylactic acid (PLA) and polycaprolactone (PCL) [9–11]. Although the fibers produced by 3D printing were relatively large (> 100 μm) for providing mechanical strength, they are not close to the scale of the extracellular matrix (ECM) or the cells (10–20 μm), thus cannot provide the cell-favorable environment for cell adhesion [12, 13]. Due to its ability to produce nanoscale fibers which is better for cell adhesion, electrospinning technology is widely used to fabricate scaffolds for simulating ECM [14–16]. However, electrospinning can only fabricate two-dimensional (2D) membranes. Although several strategies have been presented to fabricate 3D patterned electrospun nanofibrous structures [17–19], they

✉ Yong He  
yongqin@zju.edu.cn

<sup>1</sup> State Key Laboratory of Fluid Power and Mechatronic Systems, School of Mechanical Engineering, Zhejiang University, Hangzhou 310027, China

<sup>2</sup> Key Laboratory of 3D Printing Process and Equipment of Zhejiang Province, School of Mechanical Engineering, Zhejiang University, Hangzhou 310027, China

are all limited by the poor mechanical strength. Moreover, it is a challenge for the existing scaffold fabrication methods to realize accurate cell deposition, namely, they fail to obtain controlled distribution of cell density and cell types. Recently, 3D bioprinting has attracted increasing attention in tissue engineering due to its ability to fabricate complicated cell-laden structures with multiple cell types and different cell densities [20–22]. Nevertheless, the strength of hydrogel is too low to meet the requirement of long-term cell culture and induction. Therefore, here comes a question: could we realize fabrication of organ prototypes with controllable shape, nanofibrous structures, and controllable cell deposition by combining these three techniques?

Here, we presented a novel method to fabricate organ prototypes with controllable cell-laden multi-scale sheets by integrating the merits of extrusion-based 3D printing, electrospinning, and 3D bioprinting. With this method, the macroscale structures could ensure 3D shape and strength support, the nanoscale structures could offer a favorable environment for cell growth, and cells could be deposited in a controlled manner by bioprinting. In this study, we demonstrated the feasibility of this method for the manufacture of multi-scale sheets with controlled cell deposition. Cell viability, cell proliferation, and cell morphology were systematically studied compared to 2D culturing condition to confirm the excellent biocompatibility of the fabricated structures. These studies indicated that this method is superior to other approaches in that it offers an easy way to simultaneously realize the shape control, nanofibrous structures, and cell accurate deposition in fabricating organ prototypes, which may open up new potential applications in tissue engineering.

## Materials and methods

### Materials

In this study, PLA filament (PLA 1.75, Alkht Co., Ltd., Beijing, China) was used to fabricate macroscale structures, and polycaprolactone (PCL, Mw = 80,000, Solvay company) was used to fabricate nanoscale structures. Sodium alginate, gelatin, and calcium chloride (CaCl<sub>2</sub>) were purchased from Sigma-Aldrich, and alginate/gelatin hydrogel was used to encapsulate cells to realize controlled deposition on multi-scale sheets. Red dye was added to the alginate/gelatin hydrogel for visualization. MEM, ECM, FBS, and PBS were all purchased from Tangpu Biological Technology Co., Ltd., Hangzhou, China.

### Experimental setup

In order to fabricate multi-scale sheets with controlled cell deposition, a combination of three manufacturing equipments was used, as shown in Fig. 1. A extrusion-based 3D printer (D-Force 400, Trianglelab Co., Ltd., Jiangsu, China) was used to fabricate macroscale structures (Fig. 1a), a robot-controlled TL-01 electrospinning setup (Shenzhen Tongli Co. Ltd, Shenzhen, China) was used to fabricate nanoscale structures (Fig. 1b), and a 3D bioprinter (EFL-BP-6600, Suzhou Intelligent Manufacturing Research Institute, Suzhou, China) was used to print alginate/gelatin/cells (Fig. 1c).

### Fabrication process of organ prototypes with controllable cell-laden multi-scale sheets

Figure 2 shows a schematic illustration of fabrication of organ prototypes with controllable cell-laden multi-scale

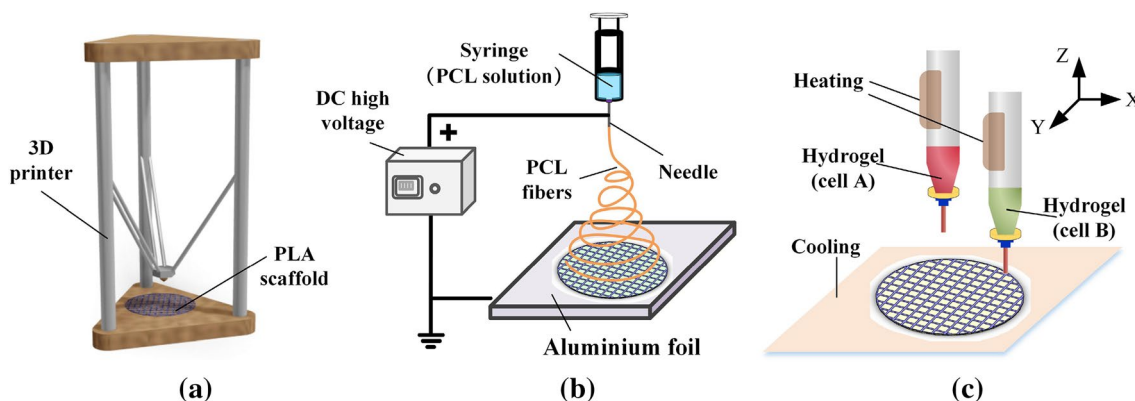


**Fig. 1** Schematic showing of the experimental setup: **a** extrusion-based 3D printer used to fabricate macroscale structures; **b** electrospinning setup used to fabricate nanoscale structures; **c** 3D bioprinter used to print alginate/gelatin/cells

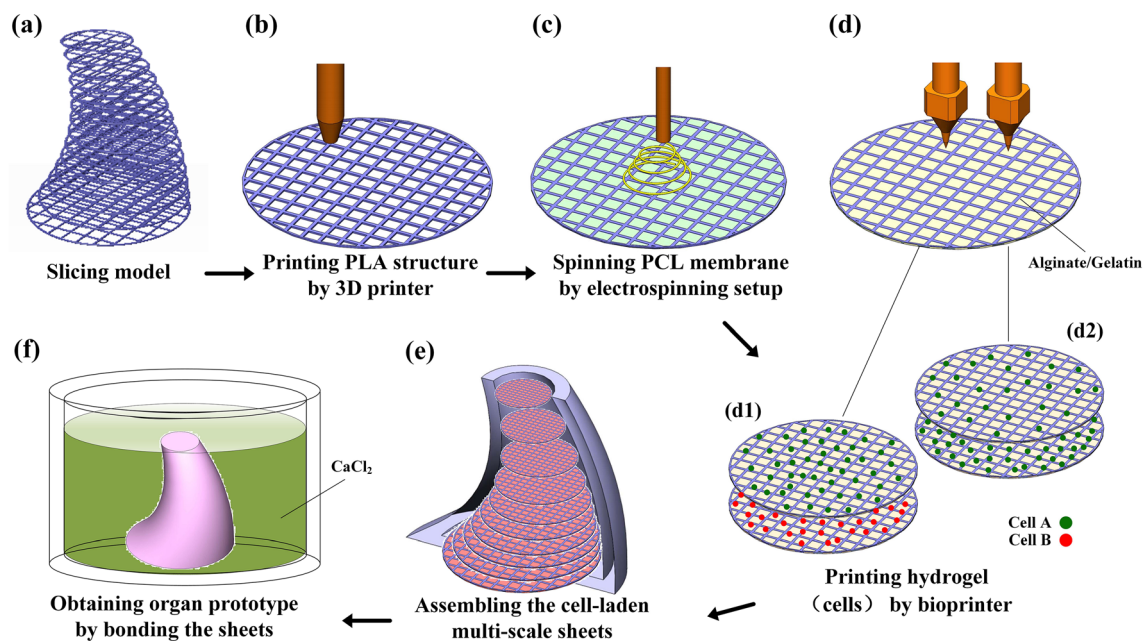


**Fig. 2** Schematic showing of fabricating organ prototypes with controllable cell-laden multi-scale sheets

sheets. First, the model was sliced to several grid structures (Fig. 2a). Then, the grid structures were fabricated by an extrusion-based 3D printer using PLA (Fig. 2b). And we used an electrospinning device to fabricate PCL nanofibrous membrane for covering the PLA structures, which resulted in a multi-scale sheet (Fig. 2c). By printing cell-laden hydrogel onto the sheets, controlled cell deposition within the multi-scale sheets was achieved (Fig. 2d). And cells of different types and concentrations can be deposited. In this process, the cell-laden hydrogel was performed by temperature cross-linking of gelatin at 4 °C. Next, the sheets consisting of PLA/PCL/Gel/cells were stacked to a 3D structure (Fig. 2e). Finally, the structure was immersed in the  $\text{CaCl}_2$  solution for complete cross-linking (Fig. 2f). In this process, the sheets were bonded together by the ionic cross-linking of alginate with calcium ion ( $\text{Ca}^{2+}$ ). Thus, organ prototypes with controllable cell-laden multi-scale sheets were obtained.

### Cell culture and cell deposition

Mouse fibroblasts (L929) and human umbilical cord vein endothelial cells (HUVECs, labeled with red fluorescent protein (RFP)) were cultured in MEM and ECM, respectively, which were added with 10% fetal bovine serum, 1% penicillin (100 units/ml), and streptomycin (100  $\mu\text{g}/\text{ml}$ ). The cells were incubated at 37 °C in 5%  $\text{CO}_2$  in polystyrene tissue culture flasks. The culture media were changed every other day, and cells were passaged using trypsin–EDTA dissociation every 4 days.

When depositing cells directly on multi-scale sheets (PLA/PCL), the sheets were first immersed in 75% ethanol under UV light for 1 h, washed three times with PBS, and incubated in 24-well plates containing culture media overnight. The cell suspensions were seeded on the sheets (one sheet in each well of 24-well plates, at  $2 \times 10^4$  cells/sheet in 1 ml MEM). The fibroblasts were incubated at 37 °C in 5%  $\text{CO}_2$ , and the media were replaced every other days.

When depositing cells on multi-scale sheets using bio-printing (PLA/PCL/Hydrogel), alginate/gelatin hydrogel was used to encapsulate cells and  $\text{CaCl}_2$  was used as cross-linking agent. The preparation process of cell-laden hydrogel solution was described in our previous study [23] and resulted in a concentration of 2% alginate ( $w/v$ ), 6% gelatin ( $w/v$ ), and a cell density of  $1 \times 10^6$  cells/ml or  $2 \times 10^6$  cells/ml. Then, cells were deposited controllably on the multi-scale sheets by bio-printing.

### Biocompatibility analysis

Cell viability was analyzed using LIVE/DEAD assay reagents (KeyGEN BioTECH Co., Ltd., Nanjing, China) according to the manufacturer's instructions. Live and dead cells were stained by calcein AM (green, 6  $\mu\text{M}$ ) and propidium iodide (red, 24  $\mu\text{M}$ ), respectively, and imaged under a confocal fluorescence microscope (ZEISS LSM780). Then, the cell viability was calculated as the number of green stained cells/total cells  $\times 100\%$  using ImageJ software.

Cell proliferation was analyzed using cell counting kit-8 (CCK-8, Dojindo) according to the manufacturer's

instructions. Different groups of cell-seeding samples were washed three times with PBS. Then, 1450  $\mu\text{l}$  MEM medium and 50  $\mu\text{l}$  CCK-8 were added to each well of 24-well plates and incubated for 3 h. Finally, the solutions were transferred to a 96-well plate (200  $\mu\text{l}$  per well) to read the OD values at a wavelength of 450 nm.

Cell morphology was analyzed by using TRITC phalloidin and DAPI to stain F-actin and nuclei, respectively, according to the manufacturer's instructions. First, the samples were fixed in 4% paraformaldehyde for 30 min, followed by permeabilized with 0.5% Triton X-100 for 5 min. Then, they were stained with TRITC phalloidin (0.1  $\mu\text{M}$ , YEASEN BioTECH Co., Ltd., Shanghai, China) for 30 min and stained with DAPI (10  $\mu\text{g}/\text{ml}$  Solarbio, Beijing, China) for 10 min. The samples were washed

three times with PBS before each step. Finally, the cell morphology was imaged under the confocal fluorescence microscope.

## Results and discussion

### Fabrication and characterization of multi-scale sheets with controlled cell deposition

According to the schematic illustration shown in Fig. 2, the actual fabrication process is shown in Fig. 3. By three steps of manufacturing, including PLA structures printing, PCL membrane spinning, and hydrogel printing, the sheets were successfully fabricated (Fig. 3a). After bonding the sheets by cross-linking alginate with  $\text{Ca}^{2+}$ , a 3D structure was fabricated, as shown in Fig. 3b.

In order to characterize the features of the fabricated structures, a sheet was fabricated as an example. By adjusting printing parameters (printing speed, layer thickness, filling rate, et al.), grid PLA structure with fiber diameter of 400  $\mu\text{m}$  and distance of 1000  $\mu\text{m}$  was printed, as shown in Fig. 4a, d. This structure could provide sufficient strength for mechanical support. The electrospun PCL fibers with 900 nm diameter covered the PLA structure to fill the pores, as shown in Fig. 4b, e. It can be seen that the nanoscale fibers effectively and equably attached to the PLA structure, which could provide a cell-favorable environment for cell growth. Figure 4c, f shows the printed fibroblasts-laden hydrogel on the multi-scale sheet. It can be seen that the cells were evenly distributed in the sheet.

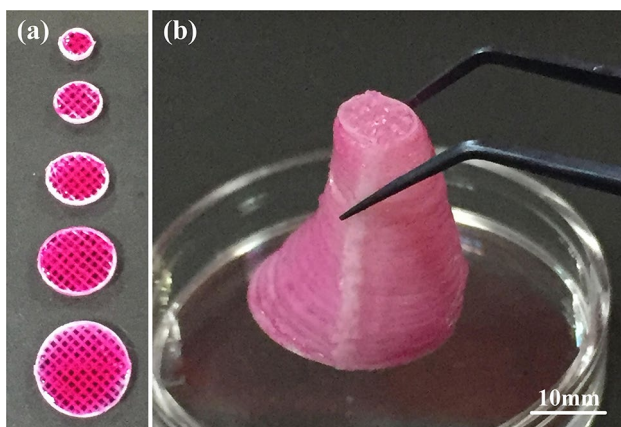


**Fig. 3** Fabrication of a 3D structure: **a** fabricated sheets; **b** 3D structure bonded by cross-linking alginate with  $\text{Ca}^{2+}$

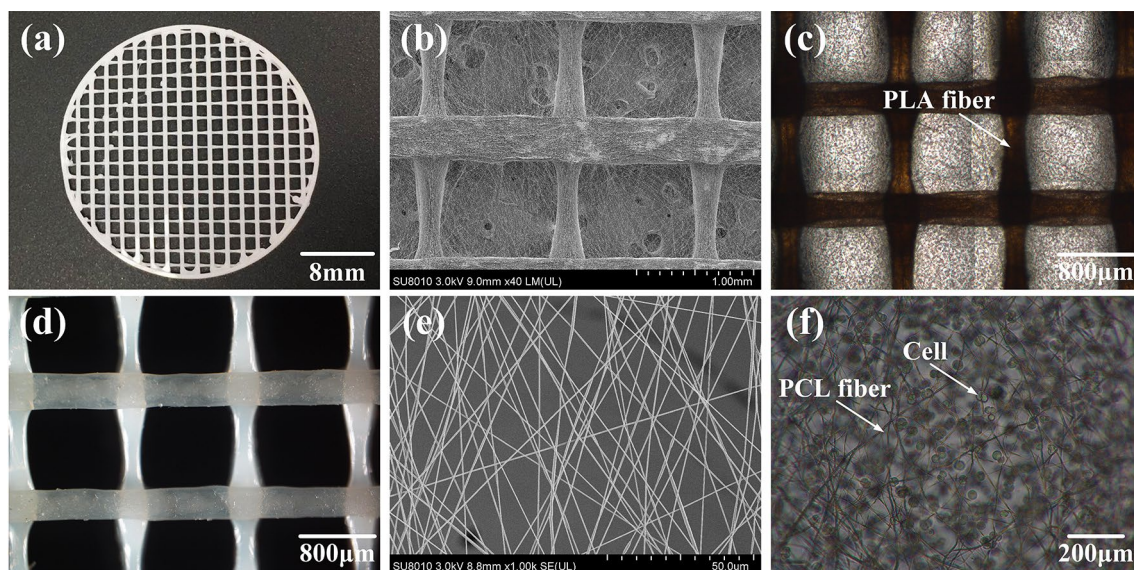


**Fig. 4** Characterization of cell-laden multi-scale sheet: **a**, **d** PLA structure; **b**, **e** PLA/PCL structure; **c**, **f** deposited cells on the multi-scale sheet

## Biocompatibility analysis of bioprinted L929 mouse fibroblasts

To evaluate the biocompatibility of the fabrication method, L929 mouse fibroblasts were mixed with alginate/gelatin hydrogel, and the mixture were deposited onto the PLA/PCL multi-scale sheet. As shown in Fig. 5a, b, most of the fibroblasts were alive (green) and a few were dead (red) through the bioprinting process. Furthermore, the cell viability analysis on day 1, 4, 7, 10 was performed to further assess the biocompatibility of the fabricated multi-scale sheet, as shown in Fig. 5c, d. The result showed that the printed fibroblasts had  $94.0 \pm 1.9\%$  cell survival after 1 day of culture,  $95.0 \pm 0.9\%$ ,  $92.3 \pm 1.0\%$ , and  $98.0 \pm 0.6\%$  survival after 4 days, 7 days, and 10 days, respectively, which confirmed that the method had a good biocompatibility. Additionally, it can be seen that the fibroblasts began to elongate on day 4, and several cells began to migrate to the sheet on day 7. This was further confirmed by the cytoskeletal staining, as shown in Fig. 5e. This behavior demonstrated that the PCL nanoscale fibers were favorable for cell growth.

Because 3D bioprinting method enabled to fabricate complex cell-laden structures with multiple cell types and controllable cell densities, we attempted to use 3D bioprinting to obtain a controllable cell deposition on the multi-scale sheet. Here, fibroblasts with density of  $1 \times 10^6$  cells/ml or  $2 \times 10^6$  cells/ml were mixed with alginate/gelatin and printed onto the multi-scale sheet, respectively. As shown in Fig. 6a, b, multi-scale sheets with different cell-seeding densities were obtained. Additionally, two types of cells, mouse fibroblasts (L929), and human umbilical cord vein endothelial cells

(RFP-HUVECs) were successfully deposited on the multi-scale sheets, as shown in Fig. 6c, d.

## Comparison of cell proliferation and cell morphology in 3D and 2D culture

In order to compare cell growth in 3D and 2D culture within the multi-scale sheets, in this study, cells cultured in the hydrogel-embedded sheets (PLA/PCL/GEL) were acted as 3D culture model, and the cells seeded on the pure multi-scale sheets without hydrogel ((PLA/PCL) and tissue culture plates (TCPS) were regarded as 2D culture model (control groups). The cell proliferation, morphology, and interaction with the fibers were investigated during the culture period.

A cell proliferation analysis using cell counting kit-8 (CCK-8) assay was performed during a 20-day culture period. As shown in Fig. 7, in the first 14 days, the proliferation rate of cells seeded on TCPS and PLA/PCL sheets was higher than that of PLA/PCL/GEL sheets. Whereas, the proliferation rate declined and the cell number decreases significantly in the control groups, while the cells in the PLA/PCL/GEL sheets continued to proliferate. This was probably because the cell contact inhibition occurred due to the limited space in 2D culture condition, while the space is enough for cell growth in 3D growth. Therefore, the PLA/PCL/GEL sheets were good for cell amplification.

Cytoskeletal observations by F-actin staining were used to determine the changes in cell morphology to study cell growth and interaction with different sheets. As shown in Fig. 8, the cells seeded on TCPS and PLA/PCL sheets showed elongated shapes in the first 5 days and changed to

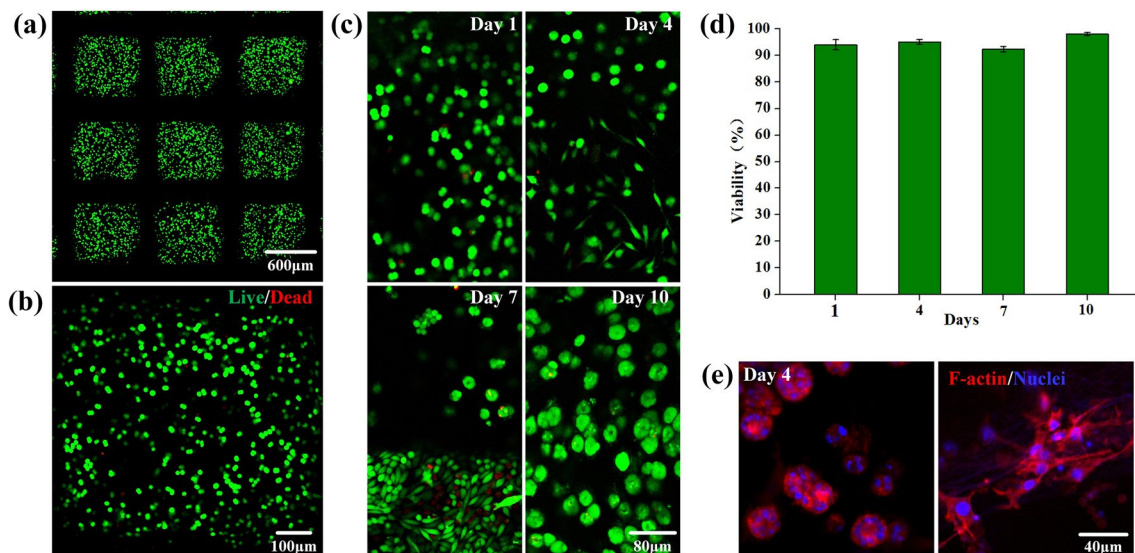


**Fig. 5** Biocompatibility analysis of bioprinted L929 mouse fibroblasts: **a**, **b** cell live/dead staining after printing; **c** cell live/dead staining on day 1, 4, 7, and 10; **d** cell viability on day 1, 4, 7, and 10 (the

error bars show mean  $\pm$ SD of 5 independent replicates); **e** cell morphology change on day 4

**Fig. 6** Cell deposition with controllable cell densities and cell types: **a** fibroblasts with density of  $1 \times 10^6$  cells/ml; **b** fibroblasts with density of  $2 \times 10^6$  cells/ml; **c** mouse fibroblasts (L929) stained with DAPI; **d** human umbilical cord vein endothelial cells (RFP-HUVECs) stained with DAPI

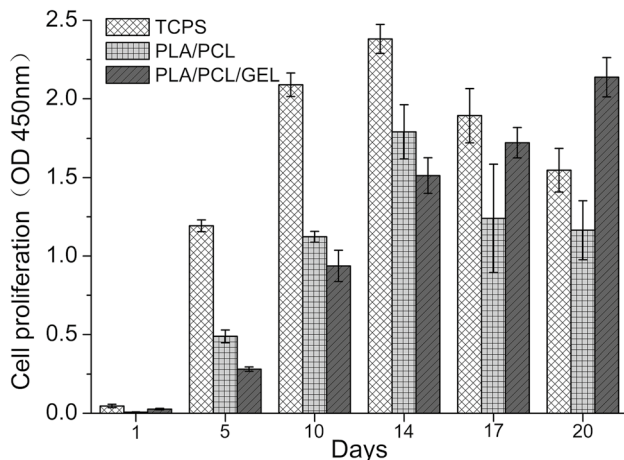
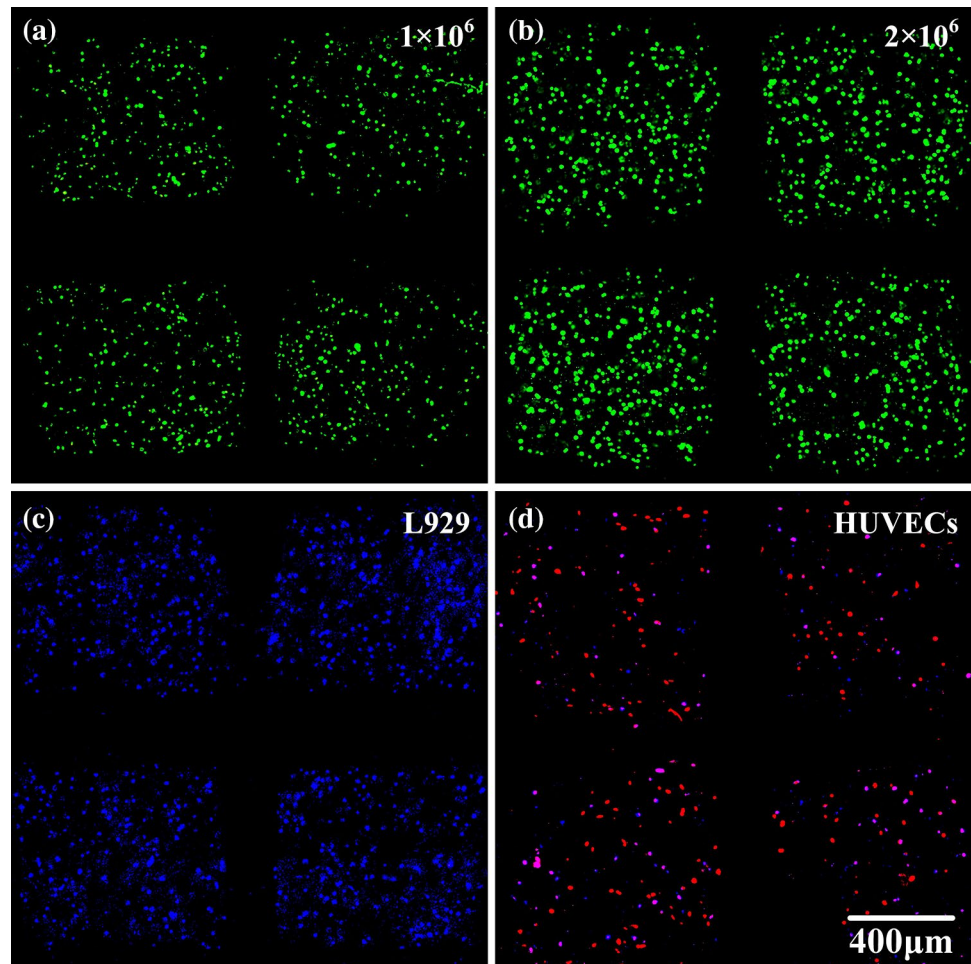


**Fig. 7** Comparison of cell proliferation between 2D culture (TCPS and PLA/PCL sheets) and 3D culture (PLA/PCL/GEL sheets)

circle shapes due to the contact inhibition and covered full of the sheet surface. Differently, the cells cultured in the PLA/PCL/GEL sheets showed spherical shapes and the diameter of the cellular spheroids gradually increased. The cellular

spheroids fused together to form a tissue. Interestingly, in the PLA/PCL/GEL sheets, the cells began to migrate to the thin PCL fibers, as shown in Fig. 9. This occurred because the cells preferred to adhere to nanoscale fibers, which could mimic the extracellular matrix (ECM). In a word, the comparison of cell proliferation and cell morphology in 3D and 2D culture confirmed the excellent compatibility of the hydrogel-laden multi-scale sheet.

### Fabrication of a multi-scale vascular structure

Recently, fabrication of a vascular structure is a hot research topic in tissue engineering. Many methods have been reported to fabricate vascular structures, including electrospinning vascular scaffolds [24, 25] and bioprinting cell-laden hydrogel-based vascular structures [26–28]. However, it is very difficult to accurately seed cells on the electrospun vascular scaffolds, and hydrogel-based vascular structures have poor mechanical strength. Here, using the presented method, we attempted to fabricate a multi-scale branched vascular structure, illustrated in Fig. 10a. According to the fabrication process described in “Fabrication process of

**Fig. 8** Comparison of cell morphology change within different structures: **a** TCPS; **b** PLA/PCL sheets; **c** PLA/PCL/GEL sheets

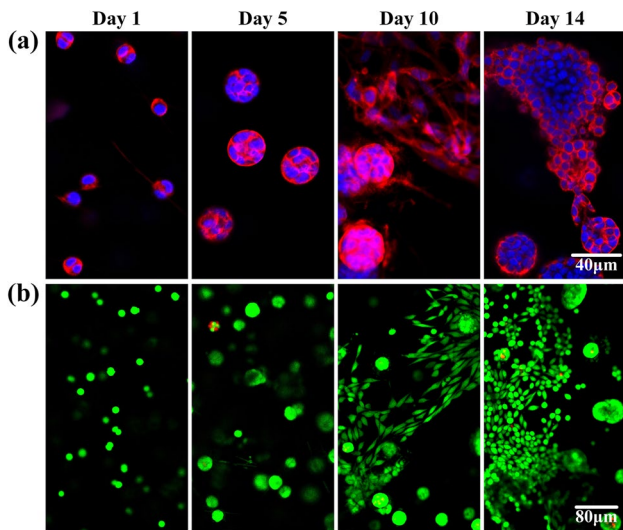
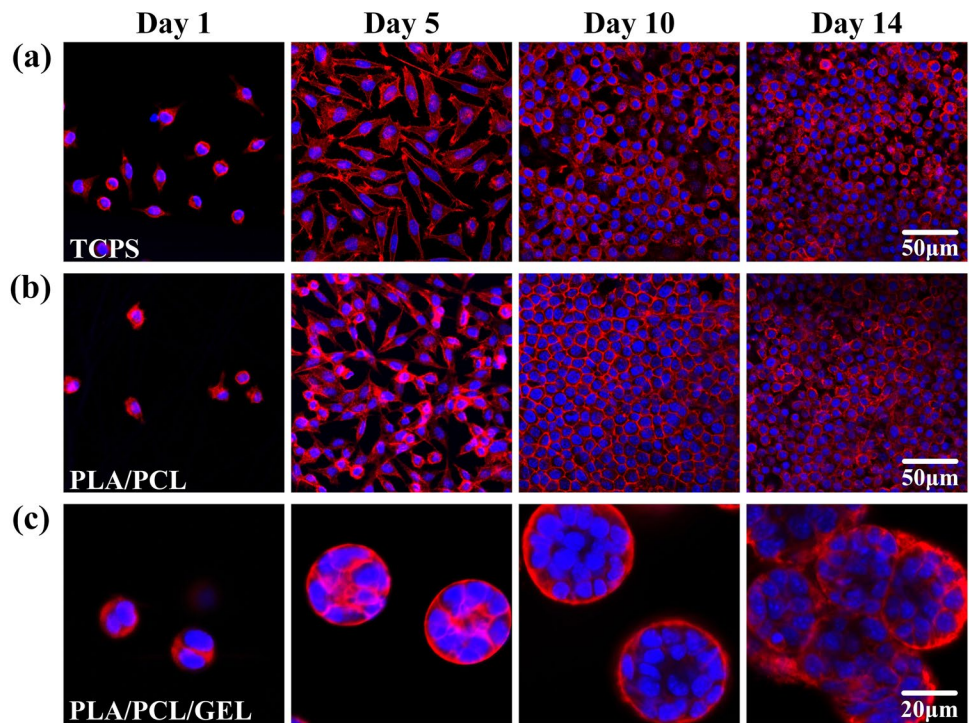


**Fig. 9** Phenomenon of cell migration to PCL fibers: **a** F-actin staining; **b** live/dead staining

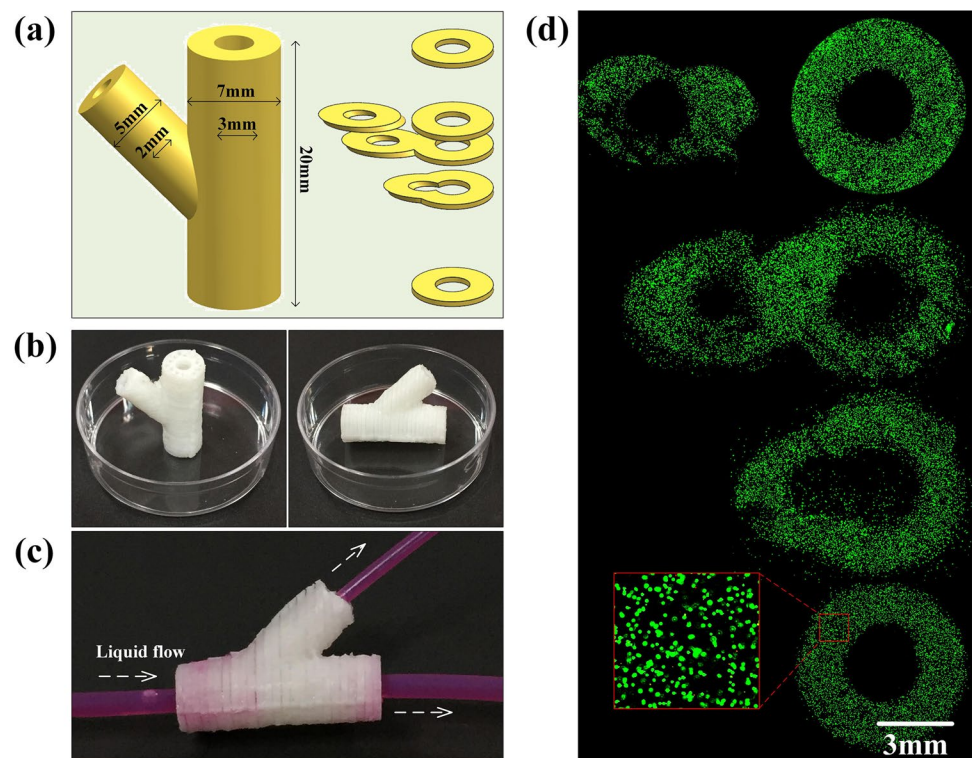
organ prototypes with controllable cell-laden multi-scale sheets” section, the multi-scale branched vascular structure was successfully fabricated, as shown in Fig. 10b. Next, a perfusion test was performed by pumping cell culture media (MEM) using a syringe pump into the fabricated vascular structure, as shown in Fig. 3c, and the result shows that the cell culture media were perfused through the channel smoothly, which demonstrated that the structure was tightly

bonded. Furthermore, L929 fibroblasts were encapsulated in the structure, and the result shows that the cells evenly distributed in vascular structures, and the fluorescent images show that almost all of the cells were alive (green). In future studies, three types of vascular cells including fibroblasts, smooth muscle cells, and endothelial cells could be deposited on the multi-scale vascular structure for better simulation of real vascular structures.

### Conclusions

In this study, a novel method in which organ prototypes with controllable shapes, nanofibrous structures, and cell deposition was fabricated layer by layer by combining the technology of extrusion-based 3D printing, electrospinning, and bioprinting. In this structure, the macroscale structures could offer 3D shape and strength support, the nanoscale structures could offer a favorable environment for cell growth, and cells could be deposited in a controlled manner by 3D bioprinting. Through systematic experiments, we have demonstrated the feasibility of this method for the manufacture of organ prototypes with cell-laden multi-scale sheets and confirmed the excellent compatibility of the hydrogel-laden multi-scale sheets. Additionally, the success of manufacturing a branched vascular structure further confirmed the stability and versatility of this method. We believe that the hybrid fabrication of multi-scale sheets with controlled cell

**Fig. 10** Fabrication of a multi-scale vascular structure: **a** a designed branched vascular model; **b** fabricated multi-scale branched vascular structure; **c** perfusion of cell culture media into the vascular structure; **d** cell culture within the vascular structure



deposition will have wide applications in manufacturing organ prototypes.

**Acknowledgements** This work was sponsored by the National Nature Science Foundation of China (Nos. 51805474, 51622510, U1609207), the Science Fund for Creative Research Groups of National Natural Science Foundation of China (No. 51821093), and China Postdoctoral Science Foundation (No. 2017M621915).

### Compliance with ethical standards

**Conflict of interest** Q.G, P.Z, R.Z, P.W, J.F and Y.H declare that they have no conflict of interest.

**Ethical approval** This paper does not contain any studies with human or animal subjects performed by any of the authors.

### References

- Visser J, Melchels FPW, Jeon JE et al (2015) Reinforcement of hydrogels using three-dimensionally printed microfibrils. *Nat Commun* 6:6933
- Laronda MM, Rutz AL, Xiao S et al (2017) A bioprosthetic ovary created using 3D printed microporous scaffolds restores ovarian function in sterilized mice. *Nat Commun* 8:15261
- Shao H, Ke X, Liu A et al (2017) Bone regeneration in 3D printing bioactive ceramic scaffolds with improved tissue/material interface pore architecture in thin-wall bone defect. *Biofabrication* 9(2):025003
- Liu A, Sun M, Shao H et al (2016) The outstanding mechanical response and bone regeneration capacity of robocast dilute magnesium-doped wollastonite scaffolds in critical size bone defects. *J Mater Chem B* 4(22):3945–3958
- Surmeneva MA, Surmenev RA, Chudinova EA et al (2017) Fabrication of multiple-layered gradient cellular metal scaffold via electron beam melting for segmental bone reconstruction. *Mater Des* 133:195–204
- Zhu C, Pongkitwitoon S, Qiu J et al (2018) Design and fabrication of a hierarchically structured scaffold for tendon-to-bone repair. *Adv Mater* 30(16):1707306
- Song J, Zhu G, Gao H et al (2018) Origami meets electrospinning: a new strategy for 3D nanofiber scaffolds. *Bio-Design Manuf* 1(4):254–264
- Zhao P, Gu H, Mi H et al (2018) Fabrication of scaffolds in tissue engineering: a review. *Front Mech Eng* 13(1):107–119
- Liu A, Xue G, Sun M et al (2016) 3D printing surgical implants at the clinic: a experimental study on anterior cruciate ligament reconstruction. *Sci Rep* 6:21704
- Ho CMB, Mishra A, Lin PTP et al (2017) 3D printed polycaprolactone carbon nanotube composite scaffolds for cardiac tissue engineering. *Macromol Biosci* 17(4):1600250
- Zein I, Huttmacher DW, Tan KC et al (2002) Fused deposition modeling of novel scaffold architectures for tissue engineering applications. *Biomaterials* 23(4):1169–1185
- Wei C, Dong J (2014) Hybrid hierarchical fabrication of three-dimensional scaffolds. *J Manuf Processes* 16(2):257–263
- Zhang B, Seong B, Nguyen VD et al (2016) 3D printing of high-resolution PLA-based structures by hybrid electrohydrodynamic and fused deposition modeling techniques. *J Micromech Microeng* 26(2):025015
- Repanas A, Andriopoulou S, Glasmacher B (2016) The significance of electrospinning as a method to create fibrous scaffolds

- for biomedical engineering and drug delivery applications. *J Drug Deliv Sci Technol* 31:137–146
15. Jun I, Han HS, Edwards J et al (2018) Electrospun fibrous scaffolds for tissue engineering: viewpoints on architecture and fabrication. *Int J Mol Sci* 19(3):745
  16. Soliman S, Sant S, Nichol JW et al (2011) Controlling the porosity of fibrous scaffolds by modulating the fiber diameter and packing density. *J Biomed Mater Res Part A* 96(3):566–574
  17. Walser J, Stok KS, Caversaccio MD et al (2016) Direct electrospinning of 3D auricle-shaped scaffolds for tissue engineering applications. *Biofabrication* 8(2):025007
  18. Gao Q, Gu H, Zhao P et al (2018) Fabrication of electrospun nanofibrous scaffolds with 3D controllable geometric shapes. *Mater Des* 157:159–169
  19. Zhao P, Cao M, Gu H et al (2018) Research on the electrospun foaming process to fabricate three-dimensional tissue engineering scaffolds. *J Appl Polym Sci* 135(46):46898
  20. Zhang B, Luo Y, Ma L et al (2018) 3D bioprinting: an emerging technology full of opportunities and challenges. *Bio-Design Manuf* 1:2–13
  21. Ying G, Jiang N, Yu C et al (2018) Three-dimensional bioprinting of gelatin methacryloyl (GelMA). *Bio-Design Manuf*. <https://doi.org/10.1007/2Fs42242-018-0028-8>
  22. Xie M, Gao Q, Zhao H et al (2018) Electro-assisted bioprinting of low-concentration GelMA microdroplets. *Small* 10:1804216
  23. He Y, Yang FF, Zhao HM et al (2016) Research on the printability of hydrogels in 3D bioprinting. *Sci Rep* 6:29977
  24. Ahn H, Ju YM, Takahashi H et al (2015) Engineered small diameter vascular grafts by combining cell sheet engineering and electrospinning technology. *Acta Biomater* 16:14–22
  25. Gong W, Lei D, Li S et al (2016) Hybrid small-diameter vascular grafts: anti-expansion effect of electrospun poly  $\epsilon$ -caprolactone on heparin-coated decellularized matrices. *Biomaterials* 76:359–370
  26. Gao Q, He Y, Fu J et al (2015) Coaxial nozzle-assisted 3D bioprinting with built-in microchannels for nutrients delivery. *Biomaterials* 61:203–215
  27. Gao Q, Liu Z, Lin Z et al (2017) 3D bioprinting of vessel-like structures with multilevel fluidic channels. *ACS Biomater Sci Eng* 3(3):399–408
  28. Shao L, Gao Q, Zhao H et al (2018) Fiber-based mini tissue with morphology-controllable GelMA microfibers. *Small* 14(44):1802187